Scholars' Mine

Spring 2016

Using adaptive thresholding and skewness correction to detect gray areas in melanoma *in situ* images

Jason R. Hagerty

Recommended Citation

USING ADAPTIVE THRESHOLDING AND SKEWNESS

CORRECTION TO DETECT GRAY AREAS IN

MELANOMA *IN SITU* IMAGES

by

JASON HAGERTY

A THESIS

Presented to the Faculty of the Graduate School of the

MISSOURI UNIVERSITY OF SCIENCE AND TECHNOLOGY

In Partial Fulfillment of the Requirements for the Degree

MASTER OF SCIENCE IN COMPUTER ENGINEERING

2016

Approved by:

Dr. R. Joe Stanley, Advisor
Dr. Randy H. Moss
Dr. William V. Stoecker

PUBLICATION THESIS OPTION

This thesis has been prepared in the style utilized by the *IEEE Transactions on Instrumentation and Measurement.* Pages 2-32 have been be formatted, submitted and accepted for publication in that journal. The Introduction and Conclusion sections have been added for purposes normal to thesis writing.

ABSTRACT

The incidence of melanoma *in situ* (MIS) is growing significantly. Detection at the MIS stage provides the highest cure rate for melanoma, but reliable detection of MIS with dermoscopy alone is not yet possible. Adjunct dermoscopic instrumentation using digital image analysis may allow more accurate detection of MIS. Gray areas are a critical component of MIS diagnosis, but automatic detection of these areas remains difficult because similar gray areas are also found in benign lesions. This paper proposes a novel adaptive thresholding technique for automatically detecting gray areas specific to MIS. The proposed model uses only MIS dermoscopic images to precisely determine gray area characteristics specific to MIS. To this aim, statistical histogram analysis is employed in multiple color spaces. It is demonstrated that skew deviation due to an asymmetric histogram distorts the color detection process. We introduce a skew estimation technique that enables histogram asymmetry correction facilitating improved adaptive thresholding results. These histogram statistical methods may be extended to detect any local image area defined by histograms.

ACKNOWLEDGMENTS

Dr. R. Joe Stanley, Dr. William V. Stoecker and Dr. Randy Moss have been my mentors and source of guidance throughout my academic and personal life. I am the result of their encouragement and expectations.

I want to thank my mother and father. Through their example and hard work, they provided me the tools I require to enable me to excel in life. They are always so proud of my accomplishments and encouraged me to strive for more.

Finally, I want to thank the person who has always believed in the man I can be. She has been the source of my strength and the reason I start everyday wanting to be a better person then I was the day before. She is both encouraging and patient with me in every aspect of my life. Erica Hagerty, I love you for everything you are and do.

TABLE OF CONTENTS

Page

SECTION

LIST OF FIGURES

LIST OF TABLES

SECTION

1. INTRODUCTION

The research presented in this thesis will aid in the diagnosing of melanoma *in situ* (MIS), the earliest stage of melanoma. Accurate detection of MIS yields the greatest chance of preventing melanoma from advancing.

To this end, the research primarily focused on the identification of gray areas in the dermoscopic image of suspected lesions. There is a correlation between lesions with observable gray areas and lesion being diagnosed as MIS. This detection of gray area alone is not a definitive method of diagnosing MIS as gray areas are also observed to a lesser extent in benign lesions. The detection of gray area first involved developing a method that was accurate despite the difference in extrinsic and intrinsic features of the dermoscopic image.

The method developed is based on a histogram analysis and identifying its skew. By using this information the lesion was adjusted so that an automatic thresholding algorithm could be applied resulting in segmented observable gray area from the dermoscopic image.

PAPER

Using Adaptive Thresholding And Skewness Correction To Detect Gray Areas In Melanoma *In Situ* Images

Gianluca Sforza, Giovanna Castellano, Sai Krishna Arika, Robert W. LeAnder, R. Joe Stanley, *Senior Member, IEEE*, William V. Stoecker, and Jason R. Hagerty

Abstract—The incidence of melanoma *in situ* (MIS) is growing significantly. Detection at the MIS stage provides the highest cure rate for melanoma, but reliable detection of MIS with dermoscopy alone is not yet possible. Adjunct dermoscopic instrumentation using digital image analysis may allow more accurate detection of MIS. Gray areas are a critical component of MIS diagnosis, but automatic detection of these areas remains difficult because similar gray areas are also found in benign lesions. This paper proposes a novel adaptive thresholding technique for automatically detecting gray areas specific to MIS. The proposed model uses only MIS dermoscopic images to precisely determine gray area characteristics specific to MIS. To this aim, statistical histogram analysis is employed in multiple color spaces. It is demonstrated that skew deviation due to an asymmetric histogram distorts the color detection process. We introduce a skew estimation technique that enables histogram asymmetry correction facilitating improved adaptive thresholding results. These histogram statistical methods may be extended to detect any local image area defined by histograms.

Index Terms—Estimation techniques, image analysis, medical imaging, melanoma *in situ* (MIS), segmentation, skewed histogram.

I. INTRODUCTION

INVASIVE and *in situ* malignant melanoma together have one of the most rapidly increasing incidence rates of all cancers. Invasive melanoma alone has an estimated incidence of 70 230 and an estimated total of 8790 deaths in the United States for 2011 [1]. 53 360 additional cases of melanoma *in situ* (MIS) are estimated for 2011 in the United States [1]. Early diagnosis at the MIS stage is of fundamental importance. MIS, unlike melanoma in the invasive stage, does not affect life expectancy [2].

One of the main diagnostic techniques is dermoscopy, a non-invasive magnification technique that enables observation of subsurface structures, improving *in vivo* diagnosis of pigmented skin lesions, as well as other diagnoses [3], [4]. In particular, contact nonpolarized dermoscopy, a variant of dermoscopy that combines optical magnification and liquid immersion to make subsurface lesion features visible, is widely used in melanoma diagnosis. With unaided dermoscopy, even in the hands of experts, diagnosis of MIS is difficult [5]. Accordingly, there is anticipation for advances in technology to allow improved detection of melanoma at the early MIS stage.

Toward this aim, image analysis techniques have been combined with contact nonpolarized dermoscopy to detect MIS structures including granularity [6], white areas [7], atypical pigment network [8], blotches [9], and solid pigment [10], among others.

The standard approach for structure analysis is to extract the lesion area using segmentation, followed by segmentation of the region of interest (ROI) containing the desired structure. Therefore, segmentation of both lesion and individual structures represents the most important stage of image analysis as it affects the accuracy of the subsequent steps. However, segmentation of dermoscopic images is difficult owing to the great variety of lesion and structure shapes, sizes, and colors, along with different skin types and textures.

To address this problem, several algorithms and techniques have been proposed for image segmentation. Thresholding, the most suitable segmentation technique, is based on a simple concept for segmenting a digital image — either grayscale or color image — into mutually exclusive regions. It is based on the assumption that adjacent pixels whose value (gray level or color value) lies within a certain range belong to the same class.

Thus, a thresholding algorithm determines a cutoff value, i.e., "threshold," chosen so that a given grayscale or color image can be binarized into a map of background and foreground pixels. The primary advantage of using thresholding techniques is that they are a computationally inexpensive method and therefore do not require a large apportionment of computational time and power. For a review of thresholding algorithms, readers are referred to [11] and [12].

Thresholding techniques have been widely investigated for segmenting lesion images. A comparison among main techniques can be found in [13]. These methods include fusion, exploiting synergy of multiple techniques for more robust final contours [14], morphology functions, and active contours (snakes) [15], gradient vector flow active contour methods [16], [17], simple thresholding followed by a wavelet packet transform [18], thresholding by the hue component of hue saturation value (HSV) color space and segmentation in red green blue (RGB) color space [19], and fuzzy C-means segmentation using an iterative-reducing mean shift algorithm [20], [21].

One main problem with thresholding algorithms is the determination of the optimal threshold, particularly if there are a large number of regions (classes) to be segmented in the image. For this reason, adaptive thresholding algorithms have been proposed to make the threshold values adaptive to the images' varied statistics. One of the pioneering algorithms for adaptive thresholding is the Otsu algorithm [22] that selects an optimal threshold using the discriminant criterion to maximize the separability of the resultant classes in gray levels. In [23], a spatially adaptive wavelet thresholding method was examined, based on context modeling, a common technique used in image compression to adapt the code to changing image characteristics. In [24], the authors used the maximization of the between-class variance and entropy as criterion functions to determine an optimal threshold for segmenting color images into nearly homogeneous regions. A combination of adaptive global thresholding segmentation and adaptive local thresholding segmentation on a multiresolution representation of mammogram color images was investigated in [25]. In [26], a method was implemented which adaptively chooses thresholds to segment objects of interest from their backgrounds using a multiscale analysis of the image probability density function. A segmentation method for detecting masses in digitized mammograms was developed in [27] using adaptive

thresholding and fuzzy entropy. Many other segmentation approaches have been proved to be useful in processing medical images [28]–[31].

In this paper, we extend dermoscopy analysis techniques by introducing a segmentation algorithm based on adaptive thresholding to detect gray areas, which are an important feature of MIS [32].

Gray color in dermoscopy images of melanocytic lesions represents melanin pigment in the upper (reticular) dermis, most frequently found in melanophages [33], [34]. Gray and gray blue areas are known to be critical structures in dermoscopic diagnosis of MIS. Gray blue areas may be most common in MIS, because they were found to be present in 76% of 37 MIS [35], but only 42% in a series that included 50% invasive melanomas contained gray areas [36]. However, gray areas are also fairly common in benign acquired nevi, particularly of the Clark (dysplastic) type [37].

The form of the gray structures is important. Gray distributed regularly in the form of a perifollicular network is commonly observed in four benign lesions: areas of solar lentigo/initial seborrheic keratosis, lichen planuslike keratosis, and pigmented actinic keratosis, all of which are more common than MIS [38]. Gray or blue gray is distributed as pepperlike granules in MIS [34]. Dark gray distributed in rhomboidal structures is also present in MIS [39]. Blue structures, because of the Tyndall effect, are found deeper in the skin than the gray areas. However, there is considerable overlap; as a result, gray and blue gray are often referred to as a single class. Additionally, the malignant gray areas are of different sizes, hues, and distribution while also mimicked by any of the aforementioned classes of benign lesions.

Because of the challenge of identification of gray area without instrumentation, automatic color analysis may afford earlier detection of these gray areas and consequently earlier detection of MIS. To the authors' knowledge, the detection of gray areas using image analysis techniques has not been explored so far.

In our pilot study [40], we proposed an approach for automatic thresholding of gray areas to be used in conjunction with contact dermoscopy. Specifically, we proposed a statistical histogram analysis approach using the hue saturation brightness (HSB) color space to derive the relationship between the skewness and the mean of the brightness color plane histogram. This relationship leads to a mean shift rule that enables histogram

asymmetry correction facilitating improved adaptive thresholding of gray area regions within a skin lesion image. Segmentation of skin lesion images using mean shift has been proposed in the previous literature (see, for example, [17]).

In this paper, the skewness correction method presented in [40] is employed in multiple color spaces and applied to a larger image set. Through a quantitative comparison between the proposed skew-corrected thresholding and a compendium of state-of-the-art basic adaptive thresholding methods, it is demonstrated that skew deviation due to an asymmetric histogram distorts the color detection process, leading to great errors in final segmentation. Application of skew correction greatly improves segmentation of gray areas.
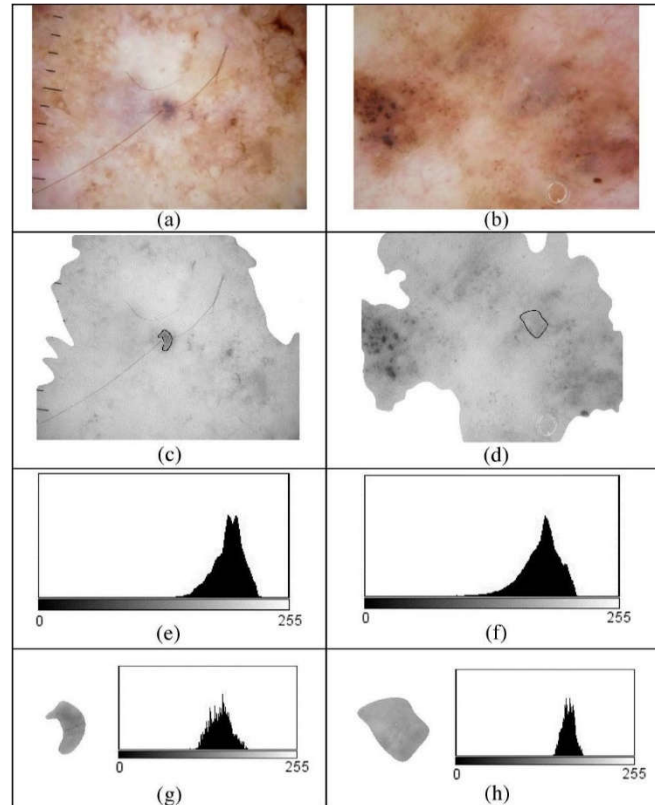
Fig 1. (a and b) Two examples of skin images, (c and d) their brightness planes with ROIs outlined, and (e and f) the corresponding histograms and (g and h) ROIs manually extracted from the two images with their brightness histograms.

II. BASIC ADAPTIVE THRESHOLDING AND INACCURACY DEFINED FOR OPTIMAL ROI DETECTION

Given a set of MIS color dermoscopy images, we considered three commonly used color spaces: RGB, $La*b*$, and HSB [41]. For each color space, all planes were analyzed for a total of nine color planes. In the following section, we take the brightness (B) plane in the HSB color space as an example.

To perform basic adaptive thresholding, we determine the average M and the standard deviation over the brightness histogram of the entire lesion area, shown in Fig. 1(e) and (f). The goal is to find a sufficient threshold range, namely, a subset of the given entire ROI range = $Range$, which is adaptable, meaning that it is proportional to the standard deviation of pixels in the B plane within a given lesion and is centered on M for that lesion. Since $Range$ varies from image to image, it is best represented as the least multiple of standard deviations that maximizes the inclusion of pixels within all ROIs (Fig. 2) within the image set.

Fig 2. Segmentation results of images in Fig. 1(a) and (b) using the interval [80, 180] for thresholding.

A series of k equal threshold intervals is determined[1] over *Range*. The ith thresholding interval, for $i = 1, \ldots, k$, is given formally by

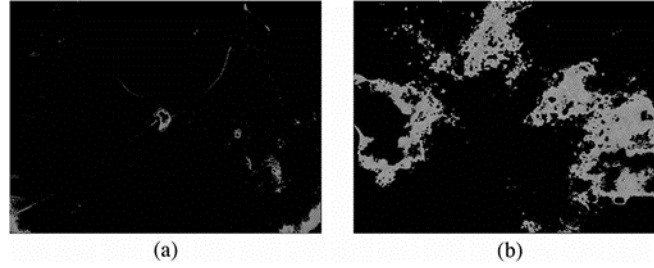$$Interval\ i = \left\{ M \quad \frac{1}{2} Range + \frac{i\ 1}{k} Range, M \quad \frac{1}{2} Range + \frac{i}{k} Range \right\} \quad (1)$$

For each threshold interval i in a given color plane, thresholding is applied to generate binary masks. All pixels in the masks generated are counted. Counts are made for the following four classes of pixels [42]:

$$Pixels\ wit\ in\ ROI = True\ Positive\ (TP)$$
$$Pixels\ missed\ wit\ in\ ROI = Fase\ Negative\ (FN)$$
$$Pixels\ outside\ ROI = False\ Positive\ (FP)$$
$$Pixels\ missed\ outside\ ROI = True\ Negative\ (TN).$$

$$(2)$$

A simple signal-to-noise ratio would be TP/FP, considering the ratio of pixels inside the desired ROI to be signal and those outside the ROI to be noise [43]. This metric has the disadvantage of scoring masks having few false positives too high and masks having few false negatives too low. Our real goal is to find the highest fraction of the ROI possible and, at the same time, the lowest fraction of the area outside the ROI possible, which is equivalent to minimizing the sum of two errors:

1) the error within the ROI, namely, $FN/(FN + TP)$;

2) the error outside the ROI, namely, $FP/(FP + TN)$.

Thus, we introduce a new error measure termed *INACCURACY,* defined as

$$INACCURACY = \frac{FN}{FN + TP} + \frac{FP}{FP + TN} \quad (3)$$

---

[1] A value of k large enough to obtain optimization, as shown in Fig. 7, is chosen. For this study, the number of threshold intervals is fixed to $k = 10$.

INACCURACY is totaled over all images and measured over all thresholds and all planes.

One main difficulty using basic adaptive thresholding was to decide the upper and lower bounds of *Range*, which varied widely among images. Accordingly, the basic adaptive thresholding method was modified as described in the following section.

III. OPTIMIZATION OF BASIC ADAPTIVE THRESHOLDING USING SKEWNESS CORRECTION

The principal idea underlying our approach is to adjust the limits of a given gray area thresholding interval and modify these limits using the skewness information associated with gray area histograms in order to improve thresholding results.

We consider the color information represented in the HSB color space as an example. In particular, we focus on the brightness component (*B* plane) that carries most of the information for the color gray [44], [45]. Fig. 1(a) and (b) shows two examples of the dermoscopy images under study. On each image, the contour of the ROI inside the MIS has been drawn by a dermatologist. The aim of our work is to find a way to automatically detect the ROI inside the MIS image.

We started from an analysis of the brightness histogram of the ROI. For 49 images, using a mask previously sketched by the dermatologist, we selected the melanoma area from the entire skin image [Fig. 1(c) and (d)], together with the ROI [bordered region in Fig. 1(c) and (d)], and we observed the corresponding brightness histograms [Fig. 1(e) and (f)]. It can be noted that, in most cases, the brightness values of the melanoma ROI covers the interval [80, 180]. Therefore, one straightforward rule for performing thresholding is to consider such an interval. Nevertheless, performing a segmentation process by simply using this interval for thresholding may generate a large false positive area, as shown in Fig. 2(b).

It is therefore necessary to reduce the size of the interval so as to capture only the most significant values from the brightness histogram, which are useful to identify the lesion's ROI. To this aim, in [40], we proposed a statistical approach to better determine the *Range* by automatically selecting a proper interval of brightness values starting from the

entire interval [0, 255]. In the following, we report the details of our approach.

Formally, the problem is to determine two variables *a* and *c,* such that the brightness values of the ROI lie in an interval that is shared by all the images in the considered data set

$$[LB, UB] = [M \quad a(S), M + c(S)] \tag{4}$$

where *LB* and *UB* are the lower bound and the upper bound of the interval, respectively, *M* is the mean of the histogram for the ROI, and *S* is the standard deviation. To estimate the values of *a* and *c* for all the available images, we examine their brightness information. Each one of the 256 bins in the brightness histogram is a tabulation of how many pixels correspond to that gray level, so the area of the image can be found by adding all the bins. Therefore, subsequent sums of the bins identify subareas of the whole image (i.e., how much area is caught by a given subset of bins). The successive sums of the pixels in the bins constitute the so-called *cumulative histogram* of the gray area. Let g_i and b_i denote the histogram values of bin *i* for each gray area and the entire lesion, respectively. To evaluate the weight that each gray area's cumulative histogram at bin g_i has relative to the entire image, we calculate the ratios between gray-level subareas and the lesion's area as

$$r_i = \frac{\sum_{j=1}^{i} g_j}{\sum_{j=1}^{255} b_j} \quad , \quad i=0,\ldots,255. \tag{5}$$
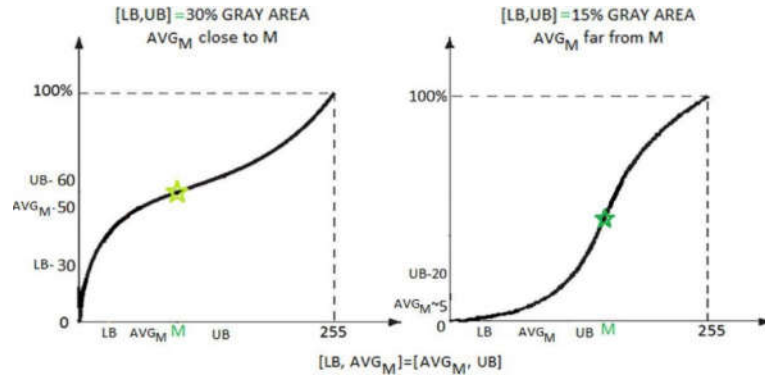

Fig 3. Cumulative histograms. It can be seen that LB and UB depend on the distance between actual and AVG_M values.

We found it useful to calculate the set of relative values for the ratios as the differences $(r_{i+1} \quad r_i)/\sum_{j=1}^{255} r_j$, where $r_{256}=0$, to represent the gain of gray area between a weighted partial sum of bins and the successive sum of bins. This helps to find the values of the bins that limit a given quantity of gray area, namely, the lower and upper bounds.

The next step is to calculate the intersection between all possible values for *LB* and *UB* extracted from all images in the set, in order to find a common set of values for thresholding the gray area that is present in a dermoscopy image. Hence, we statistically model the variables *a* and *c*. The whole process is summarized as follows.

First, we collect the mean for every gray area histogram; then, the average of all these values is found. We indicate this value with AVG_M (see Fig. 3). Second, selecting the point AVG_M as a midrange for the desired *LB* and *UB* and going one step forward and one step backward from it, we consider those bins that bound 30%, 50%, and 90% of the gray area. The ideal position for a histogram is to have its mean *M* at the point AVG_M, because, then, the interval [*LB, UB*] surrounding AVG_M will be sufficiently narrow and close to the main bins, thereby detecting a gray area. On the contrary, we observed that the value of the actual mean *M* is far from AVG_M and that the interval becomes larger. The intersection of these intervals over the image set yields a restricted region which will not threshold a sufficient amount of gray area for the histograms, with means far from its expected value AVG_M.

Therefore, the problem becomes finding a common thresholding interval that evaluates, for each image, the amount that the point AVG_M should be shifted to yield the actual mean *M*. To do this, we consider the *skewness* of the histogram distribution, because of its statistical relevance in describing a distribution. By measuring the skewness of the distributions, we empirically evaluated the trend of these curves [46], [47]. We found that left/right skewed curves of a histogram generate two different curves for the relative ratios.
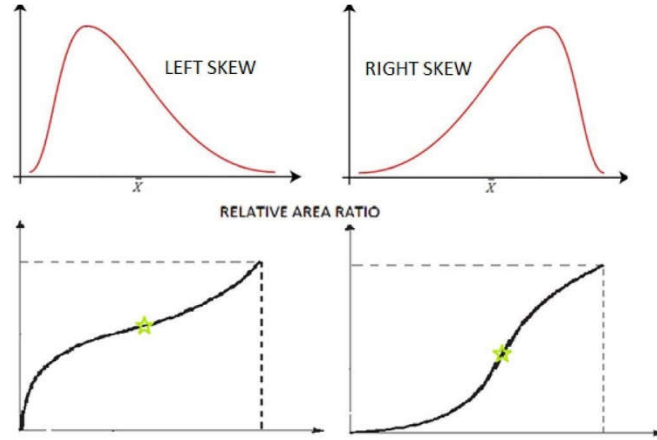
Fig 4. Relative ratios for differently skewed histograms: The mean case.

In Fig. 4, one can observe that the relative ratio corresponding to the mean of the original histogram (marked by a star) has different values, in the case of a left- or a right-skewed curve. This means that the amount of gray area detected at a given threshold varies with the skewness. This is particularly true in the case of very skewed histograms: In such a case, the difference between the actual mean M and the AVG_M is so consistent that the shared interval $[LB, UB]$ could not detect any gray area from those images. Particularly for those cases, it is essential to find the relationship between the difference $M - AVG_M$ and the skewness of the gray area's histogram. Using the well-known formula for skewness [48]

$$sk = \frac{M - mode}{S} \qquad (6)$$

we observe that M equals AVG_M when the following conditions hold.

1) $mode = AVG_M$.

2) $sk = 0$.

3) $S = any\ value$.
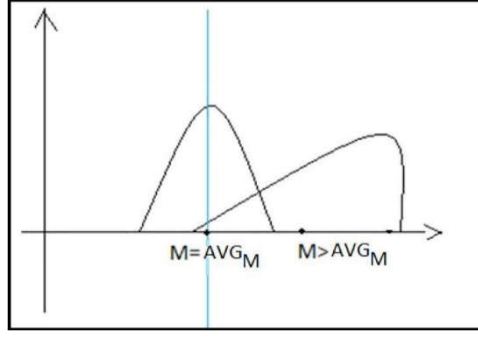
Fig 5. Locating the mean of a skewed distribution. The difference M AVGM is critical as it determines skew.

Of course, this condition is satisfied by any symmetric distribution, including all Gaussian distributions with the mean centered at AVG_M.

Let AVG_M be the ideal point to be shifted. It may be considered as the axial center of a Cartesian plane with the ordinate axes shifted from the origin toward AVG_M (see Fig. 5). Then, for a generic distribution lying over such a new plane, we can find new statistics that are relative to the original plane. Its relative mean is

$$M_{rel} = M \quad AVG_M \tag{7}$$

and its relative mode is

$$mode_{rel} = mode \quad AVG_M. \tag{8}$$

Thus, we have a value also for the relative skewness sk_{rel}, which is the skewness calculated with respect to the symmetric histogram centered at AVG_M

$$
\begin{aligned}
sk_{rel} &= sk \quad sk_{AVG_M} \\
&= \frac{(M \quad AVG_M) \quad (mode \quad AVG_M)}{S}
\end{aligned}
\tag{9}
$$

Now, we observe that $sk = 0$ if $(M = AVG_M)$, as it is the skewness of a symmetric distribution. Accordingly, we have

$$M \quad AVG_M = sk(S) + (mode \quad AVG_M). \tag{10}$$

Equation (10) calculates the shifting value for AVG_M to be moved to find the actual mean M of a histogram distribution.

IV. SEGMENTATION ALGORITHM USING SKEW TECHNIQUE

The shifting quantity derived from the approach described in Section III can be applied to perform an adaptive thresholding useful in identifying a ROI in dermoscopy images. First, a common interval for thresholding all the image set is identified. Then, such interval is adapted to each image to achieve improved results.

The segmentation algorithm is described as follows using the brightness image of the whole skin.

1) Determine the lesion histogram and the distance of its average from the central bin (128), denoted by $DIFF$.

2) Shift the gray area histogram by $DIFF$; find its cumulative histogram, and weight its bins using the total area of the lesion; save the differences between these values, namely, the relative area ratios—as the gain of gray area that is between one weighted partial sum and the successive partial sum.

3) From the relative ratios of the entire image set, find a common range of values that catch the X% of gray area ($X = 30$, 60, or 90); shift this range by the result of (10), and find the appropriate thresholds for a specific image in the brightness plane.

The image in Fig. 1(b) has been taken as an example to show how $INACCURACY$ improves using the skew correction. The first line in Fig. 6 is an illustration of Fig. 1(b) processed with this algorithm. In particular, the second image in line represents the thresholding result before the shift ($INACCURACY = 0.969$), and the third image in the line represents the thresholding result after the shift ($INACCURACY = 0.819$).

Summarizing, we found the mean of a gray area distribution to be the best parameter for localizing the core of the gray area. This process therefore generates an interval for thresholding the core of gray area that is present inside a dermoscopy image of a MIS.

V. EXPERIMENTS AND RESULTS

The segmentation algorithm and error measure described in the previous sections were used to improve the automatic detection of the gray ROI inside the melanoma image.

A. Instrumentation and Images

The contact dermoscopy instrumentation used in this study is the 3Gen DermLite Fluid attachment (3Gen LLC, San Juan Capistrano, CA). It employs ten-power magnification with bright white LED lighting and a gel interface. All images were acquired with a Sony DSC-W70 7.2-megapixel digital camera with dermoscopic adapter.

A set of 121 MIS images was obtained in the study SBIR R44 CA-101639-02A2 of the National Institutes of Health and approved by the Phelps County Regional Medical Center Institutional Review Board, Rolla, MO, under the guidelines of the Belmont Report. Among the 121 images of the data set, 49 were found to have gray regions and considered as MIS for segmentation. Gray regions were manually extracted by a dermatologist. Specifically, the border contour of each MIS and the contour of the most identifiable gray ROI inside each MIS were drawn by the dermatologist using a second-order spline technique [5].

B. Segmentation Results

In this section, we show examples of segmentation results by applying both a thresholding with a fixed interval and an adaptive thresholding with the skew correction given in (10). For experiments, we used JavaScript supported by the ImageJ software environment v.1.4.2 [49] for converting images in different color spaces and Matlab R2009b to implement the thresholding algorithm.

Fig. 6 compares the segmentation result of five images using a fixed thresholding interval and using the adaptive thresholding interval with skew correction. It can be seen that no gray area is detected by applying a thresholding with a fixed interval. Conversely, a gray area centered in the ROI is detected by applying the skew-corrected thresholding interval.
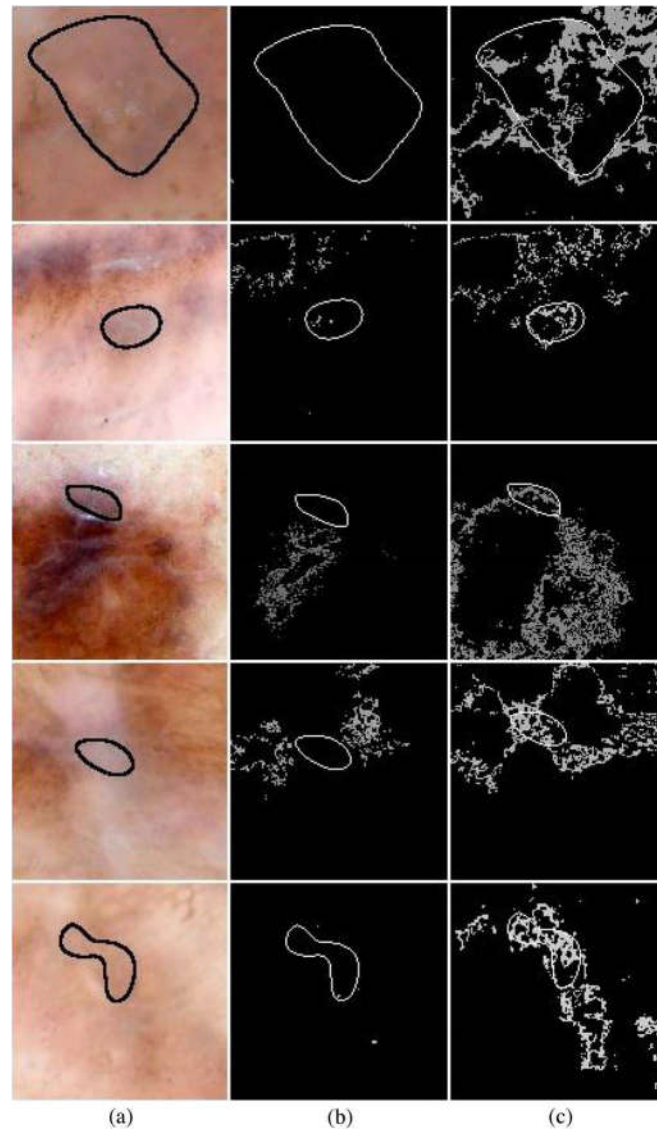

Fig 6. (a) Zoom on original color images with ROI manually drawn. (b) Segmentation result with fixed thresholding interval. (c) Segmentation result with adaptive skew-corrected interval.

To better evaluate the effect of the proposed skew correction technique, thresholding was performed on six color planes taken from different color spaces, namely, the planes a^*, b^*, L, green, blue, and B (brightness). Using the basic adaptive thresholding, the per-lesion average $INACCURACY$ taken over the 49 images was determined for each of ten threshold intervals (channels) and for each of the six color planes. Results are shown in Fig. 7. It can be seen that the best average $INACCURACY = 0.432$ was obtained for the b^* plane. With the skew-corrected thresholding, the average $INACCURACY$ for the 30% brightness plane was 0.670, while the best $INACCURACY$ (0.302) was obtained at 90% brightness.

We noted that the basic adaptive thresholding results are fairly close across threshold intervals and across color planes. In contrast, the skew-corrected thresholding clearly obtained the best $INACCURACY$ results. This is because skew correction is not automatically applied to all images. It optimizes the thresholding interval for each image, rather than finding an optimum interval for all images, as the basic adaptive thresholding technique does. The skew correction thus yields an estimate for the minimum error achievable by histogram correction.

Finally, our thresholding method was compared against the basic adaptive version, as well as a compendium of 16 thresholding methods [50] applied to the five images shown in Fig. 6. Comparative results in terms of $INACCURACY$ are shown in Table I. It can be seen that the proposed skew-corrected thresholding provides, in most cases, lower $INACCURACY$ values than the other methods. In terms of average $INACCURACY$ computed on the considered images (last column in the table), our method compares very favorably with all the other methods.
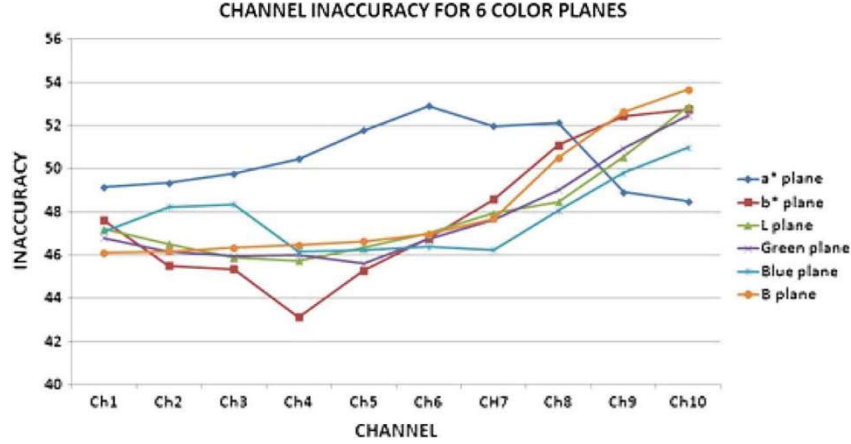
Fig 7. INACCURACY versus threshold interval channel, using basic adaptive thresholding on six color planes.

VI. CONCLUSION

This paper has demonstrated that adaptive threshold determination using skewness correction can provide more accurate gray area detection. Based on the metric *INACCURACY,* correction of the estimated histogram asymmetry deviation allows significant improvement of gray area segmentation. Even though the technique reported here has been applied only to dermoscopic images, the derived statistical framework is independent of the chosen domain. Consequently, it may be used to perform segmentation of any kind of digital medical images.

This study was motivated by the discovery that the histograms of gray areas are heterogeneous, with a minority having a blue "tail" skewed primarily to the right. These blue tails likely represent dermatologists' assessment that gray and blue-gray have the same physiology. This assessment includes gray with blue-gray because the gray is at a deeper level in the skin, resulting in more blue due to the Tyndall effect. Consequently, a set of images having gray is heterogeneous, with the gray areas in some images having a histogram skewed toward brighter blue. We conclude that both gray and blue gray are seen in these early melanomas with some images having greater amounts of blue, resulting in a rightward skew [34].

Results from this study were determined for only a small number of images. The proposed methods will be applied to a larger set, again using adaptive thresholding and comparing skew-corrected segmentation with uncorrected segmentation.

The presented comparative results show that thresholding without the proposed skew correction can lead to great errors in final segmentation. One possible explanation is that existing thresholding methods are primarily designed for segmentation of easily visible and detectable structures, whereas our method can yield accurate segmentation of small ROI that is not clearly delineated. Correct segmentation of these regions depends entirely upon histogram analysis, and it is therefore quite sensitive to skew distortion of the image histograms. Further research could combine the proposed histogram analysis with one or more existing thresholding methods to provide further improvements in existing segmentation results.

The challenging task of gray area segmentation comprises another step toward the development of an automatic diagnostic system capable of detecting the early stages of melanoma from a set of features extracted from dermoscopic images.

Finally, we emphasize that reliable identification of MIS in the clinic has not yet been demonstrated. Particularly for critical objects which are only approximately determined by humans, such as location on the gray-to-blue-gray spectrum, new analytic techniques may be employed using instrumentation to effect more precise early melanoma discrimination. As Lucas *et al.* noted, up to 36% of MIS might be overlooked and not detected until a subsequent follow-up visit. This might be the case, even when dermoscopy, clinical information, and monitoring for change with total body photography are combined [5]. As Lucas *et al.* predicted, "possibly, future technologies will be developed that will be able to discriminate aberrant growth patterns even in these early *in situ* lesions" [5].

TABLE 1.

INACCURACY COMPARISON BETWEEN THE SKEW CORRECTION METHOD
AND OTHER THRESHOLDING METHODS ON IMAGES IN FIG. 6

METHOD	IMAGE 1	IMAGE 2	IMAGE 3	IMAGE 4	IMAGE 5	AVG
Skew correction	0.455	0.439	0.210	0.165	0.212	0.296
Basic adaptive	0.907	1.025	0.541	0.982	0.821	0.855
IJ-IsoData [50]	0.425	0.516	0.254	0.699	0.415	0.462
Huang [51]	0.416	0.750	0.725	0.491	0.670	0.610
Intermodes [52]	0.993	0.733	0.991	0.678	0.753	0.830
IsoData [53]	0.425	0.614	0.342	0.693	0.455	0.506
Li [54]	0.407	0.633	0.574	0.681	0.517	0.562
MaxEntropy[55]	0.926	0.721	0.657	0.681	0.200	0.637
Mean [56]	0.500	0.682	0.574	0.336	0.539	0.526
MinError [57]	0.500	0.682	0.878	0.984	0.539	0.716
Minimum [52]	0.993	0.721	0.911	0.677	0.791	0.835
Moments [58]	0.425	0.474	0.296	0.639	0.434	0.454
Otsu [22]	0.412	0.633	0.482	0.698	0.475	0.540
Percentile [59]	0.575	0.724	0.574	0.442	0.562	0.575
RenyiEntropy [55]	0.925	0.721	0.654	0.681	0.200	0.636
Shanbhag [60]	0.410	0.721	0.574	0.677	0.455	0.567
Triangle [61]	0.909	0.913	0.638	0.698	0.872	0.806
Yen [62]	0.925	0.721	0.656	0.681	0.213	0.639

ACKNOWLEDGMENT

REFERENCES

[1]   R. Siegel, E. Ward, O. Brawley, and A. Jemal, "Cancer statistics, 2011. The impact of eliminating socioeconomic and racial disparities on premature cancer deaths," *Cancer J. Clinic.*, vol. 61, no. 4, pp. 212–236, Jul./Aug. 2011.

[2]   S. Mocellin and D. Nitti, "Cutaneous melanoma *in situ*: Translational evidence from a large population-based study," *Oncologist*, vol. 16, no. 6, pp. 896–903, 2011.

[3] G. Argenziano, H. P. Soyer, S. Chimenti, R. Talamini, R. Corona, F. Sera, M. Binder, L. Cerroni, G. De Rosa, G. Ferrara, R. Hofmann-Wellenhof, M. Landthaler, S. W. Menzies, H. Pehamberger, D. Piccolo, H. S. Rabinovitz, R. Schiffner, S. Staibano, W. Stolz, I. Bartenjev, A. Blum, R. Braun, H. Cabo, P. Carli, V. De Giorgi, M. G. Fleming, J. M. Grichnik, C. M. Grin, A. C. Halpern, R. Johr, B. Katz, R. O. Kenet, H. Kittler, J. Kreusch, J. Malvehy, G. Mazzocchetti, M. Oliviero, F. Ozdemir, K. Peris, R. Perotti, A. Perusquia, M. A. Pizzichetta, S. Puig, B. Rao, P. Rubegni, T. Saida, M. Scalvenzi, S. Seidenari, I. Stanganelli, M. Tanaka, K. Westerhoff, H. Wolf, O. Braun-Falco, H. Kerl, T. Nishikawa, K. Wolff, and A. W. Kopf, "Dermoscopy of pigmented skin lesions: Results of a consensus meeting via the Internet," *J. Amer. Acad. Dermatol.*, vol. 48, no. 5, pp. 679–693, May 2003

[4] G. Argenziano, H. P. Soyer, V. De Giorgi, D. Piccolo, P. Carli, M. Delfino, A. Ferrari, R. Hofmann-Wellenhof, D. Massi, G. Mazzoccheti, M. Scalvenzi, and I. H. Wolf, *Interactive Atlas of Dermoscopy*.   Milan, Italy: EDRA Med. Pub., 2000.

[5] C. R. Lucas, L. L. Sanders, J. C. Murray, S. A. Myers, R. P. Hall, and J. M. Grichnik, "Early melanoma detection: Nonuniform dermoscopic features and growth," *J. Amer. Acad. Dermatol.*, vol. 48, no. 5, pp. 663– 671, May 2003.

[6] W. V. Stoecker, M. Wronkiewiecz, R. Chowdhury, R. J. Stanley, J. Xu, A. Bangert, B. Shrestha, D. A. Calcara, H. S. Rabinovitz, M. Oliviero, F. Ahmed, L. A. Perry, and R. Drugge, "Detection of granularity in dermoscopy images of malignant melanoma using color and texture features," *Comput. Med. Imag. Graph.*, vol. 35, no. 2, pp. 144–147, 2011.

[7] A. Dalal, R. H. Moss, R. J. Stanley, W. V. Stoecker, K. Gupta, D. A. Calcara, J. Xu, B. Shrestha, R. Drugge, J. M. Malters, and L. A. Perry, "Concentric decile segmentation of white and hypopigmented areas in dermoscopy images of skin lesions allows discrimination of malignant melanoma," *Comput. Med. Imag. Graph.— Special Dermatology Issue,* vol. 35, no. 2, pp. 148–154, Mar. 2011.

[8]   B. Shrestha, J. Bishop, K. Kam, X. Chen, R. H. Moss, W. V. Stoecker, Umbaugh, R. J. Stanley, M. E. Celebi, A. A. Marghoob, G. Argenziano, and H. P. Soyer, "Detection of atypical texture features in early melanoma detection," *Skin Res. Technol.*, vol. 16, no. 1, pp. 60–65, Feb. 2010.

[9]   A. Khan, K. Gupta, R. J. Stanley, W. V. Stoecker, R. H. Moss, G. Argenziano, H. P. Soyer, H. S. Rabinovitz, and A. B. Cognetta, "Fuzzy logic techniques for blotch feature evaluation in dermoscopy images," *Comput. Med. Imag. Graph.*, vol. 33, no. 1, pp. 50–57, Jan. 2009.

[10] A. Murali, W. V. Stoecker, and R. H. Moss, "Detection of solid pigment in dermatoscopy images using texture analysis," *Skin Res. Technol.*, vol. 6, no. 4, pp. 193–198, Nov. 2000.

[11] P. K. Sahoo, S. Soltani, and A. K. C. Wong, "A survey of thresholding techniques," *Comput. Vis., Graph. Image Process.*, vol. 41, no. 2, pp. 233– 260, Feb. 1988.

[12] N. Pal and S. Pal, "A review on image segmentation techniques," *Pattern Recognit.*, vol. 26, no. 9, pp. 1277–1294, Sep. 1993.

[13] M. Silveira, J. C. Nascimento, J. S. Marques, A. R. S. Marcal, Mendonca, S. Yamauchi, J. Maeda, and J. Rozeira, "Comparison of segmentation methods for melanoma diagnosis in dermoscopy images," *IEEE J. Sel. Topics Signal Process.*, vol. 3, no. 1, pp. 35–45, Feb. 2009.

[14] M. E. Celebi, H. Sae, H. Iyatomi, and G. Schaefer, "Robust border detection in dermoscopy images using threshold fusion," in *Proc. 17th IEEE Conf. Image Process.*, 2010, pp. 2541–2544.

[15] K. Taouil and N. B. Romdhane, "Automatic segmentation and classification of skin lesion images," in *Proc. 2nd Int. Conf. Distrib. Frameworks Multimedia Appl.*, 2006, pp. 1–12.

[16] B. Erkol, R. H. Moss, R. J. Stanley, W. V. Stoecker, and E. Hvatum, "Automatic lesion boundary detection in dermoscopy images using gradient vector flow snakes," *Skin Res. Technol.*, vol. 11, no. 1, pp. 17–26, Feb. 2005.

[17] H. Zhou, G. Schaefer, M. E. Celebi, F. Lin, and T. Liu, "Gradient vector flow with mean shift for skin lesion segmentation," *Comput. Med. Imag. Graph.*, vol. 35, no. 2, pp. 121–127, Mar. 2011.

[18] A. Chiem, A. Al-Jumaily, and R. N. Khushaba, "A novel hybrid system for skin lesion detection," in *Proc. 3rd Int. Conf. Intell. Sensors, Sensor Netw. Inf.*, 2007, pp. 567–572.

[19] R. M. Jusoh, N. Hamzah, M. H. Marhaban, and N. M. A. Alias, "Skin detection based on thresholding in RGB and hue component," in *Proc. IEEE ISIEA*, 2010, pp. 515–517.

[20] H. Zhou, G. Schaefer, A. Sadka, and M. E. Celebi, "Anisotropic mean shift based *C*-fuzzy means segmentation of dermoscopy images," *IEEE J. Sel. Topics Signal Process.*, vol. 3, no. 1, pp. 26–34, Feb. 2009.

[21] H. Zhou, G. Schaefer, and C. Shi, "Fuzzy *C*-means techniques for medical image segmentation," *Fuzzy Syst. Bioinform. Comput. Biol.*, vol. 242, pp. 257–271, 2009.

[22] N. Otsu, "A threshold selection method from gray-level histograms," *IEEE Trans. Syst., Man, Cybern.*, vol. SMC-9, no. 1, pp. 62–66, Jan. 1979.

[23] S. G. Chang, B. Yu, and M. Vetterli, "Spatially adaptive wavelet thresholding with context modeling for image denoising," *IEEE Trans. Image Process.*, vol. 9, no. 9, pp. 1522–1531, Sep. 2000.

[24] R. Harrabi and E. B. Braiek, "Color image segmentation using automatic thresholding techniques," in *Proc. 8th Int. Multi-Conf. Syst., Signals, Devices*, 2001, pp. 1–6.

[25] K. Hu, X. Gao, and F. Li, "Detection of suspicious lesions by adaptive thresholding based on multiresolution analysis in mammograms," *IEEE Trans. Instrum. Meas.*, vol. 60, no. 2, pp. 462–472, Feb. 2011.

[26] X. P. Zhang and M. D. Desai, "Segmentation of bright targets using wavelets and adaptive thresholding," *IEEE Trans. Image Process.*, vol. 10, no. 7, pp. 1020–1030, Jul. 2001.

[27] F. Younesi, N. R. Alam, R. A. Zoroofi, A. Ahmadian, and M. Guiti, "Computer-aided mass detection on digitized mammograms using adaptive thresholding and fuzzy entropy," in *Proc. 29th Annu. Int. Conf. IEEE Eng. Med. Biol. Soc.*, 2007, pp. 5638–5640.

[28] S. Delsanto, F. Molinari, P. Giustetto, W. Liboni, S. Badalamenti, and J. S. Suri, "Characterization of a completely user-independent algorithm for carotid artery segmentation in 2-D ultrasound images," *IEEE Trans. Instrum. Meas.*, vol. 56, no. 4, pp. 1265–1274, Aug. 2007.

[29] J. Hao, Y. Shen, and Q. Wang, "Segmentation for MRA image: An improved level-set approach," *IEEE Trans. Instrum. Meas.*, vol. 56, no. 4, pp. 1316–1321, Aug. 2007.

[30] M. T. A. Basile, L. Caponetti, G. Castellano, and G. Sforza, "A texture- based image processing approach for the description of human oocyte cytoplasm," *IEEE Trans. Instrum. Meas.*, vol. 59, no. 10, pp. 2591–2601, Oct. 2010.

[31] R. Chandrasekhar and Y. Attikiouzel, "New range-based neighbourhood operator for extracting edge and texture information from mammograms for subsequent image segmentation and analysis," *Proc. Inst. Elect. Eng.—Sci. Meas. Technol.*, vol. 147, no. 6, pp. 408–413, 2000.

[32] I. Zalaudek, G. Docimo, and G. Argenziano, "Using dermoscopic criteria and patient-related factors for the management of pigmented melanocytic nevi," *Arch. Dermatol.*, vol. 145, no. 7, pp. 816–826, 2009.

[33] I. Zalaudek, G. Argenziano, G. Ferrara, H. P. Soyer, R. Corona, F. Sera, L. Cerroni, A. Carbone, A. Chiominto, L. Cicale, G. De Rosa, A. Ferrari, R. Hofmann-Wellenhof, J. Malvehy, K. Peris, M. A. Pizzichetta, S. Puig, M. Scalvenzi, S. Staibano, and V. Ruocco, "Clinically equivocal melanocytic skin lesions with features of regression: A dermoscopic-pathological study," *Br. J. Dermatol.*, vol. 150, no. 1, pp. 64–71, Jan. 2004.

[34] R. P. Braun, O. Gaide, M. Oliviero, A. W. Kopf, L. E. French, J. H. Saurat, and H. S. Rabinovitz, "The significance of multiple blue-grey dots (granularity) for the dermoscopic diagnosis of melanoma," *Br. J. Dermatol.*, vol. 157, no. 5, pp. 907–913, Nov. 2007.

[35] M. A. Pizzichetta, G. Argenziano, R. Talamini, D. Piccolo, A. Gatti, G. Trevisan, G. Sasso, A. Veronesi, A. Carbone, and H. P. Soyer, "Dermoscopic criteria for melanoma *in situ* are similar to those for early invasive melanoma," *Cancer*, vol. 91, no. 5, pp. 992–997, Mar. 2001.

[36] M. Troya-Martín, N. Blázquez-Sánchez, I. Fernández-Canedo, M. Frieyro-Elicegui, R. Fúnez-Liébana, F. Rivas-Ruiz, S. Seidenari, G. Pellacani, and C. Grana, "Dermoscopic study of cutaneous malignant melanoma: Descriptive analysis of 45 cases," *Art. Spanish Actas Dermosifiliogr.*, vol. 99, no. 1, pp. 44–53, Jan./Feb. 2008.

[37] S. Seidenari, G. Pellacani, and C. Grana, "Colors in atypical nevi: A computer description reproducing clinical assessment," *Skin Res. Technol.*, vol. 11, no. 1, pp. 36–41, Feb. 2005.

[38] M. Tanaka, M. Sawada, and K. Kobayashi, "Key points in dermoscopic differentiation between lentigo maligna and solar lentigo," *J. Dermatol.*, vol. 38, no. 1, pp. 53–58, Jan. 2011.

[39] M. T. Sahin, S. Oztürkcan, A. T. Ermertcan, and A. T. Güneṣ, "A comparison of dermoscopic features among lentigo senilis/initial seborrheic keratosis, seborrheic keratosis, lentigo maligna and lentigo maligna melanoma on the face," *J. Dermatol.*, vol. 31, no. 11, pp. 884–889, Nov. 2004.

[40] G. Sforza, G. Castellano, R. J. Stanley, W. V. Stoecker, and J. Hagerty, "Adaptive segmentation of gray areas in dermoscopy images," in *Proc. 6th Int. Symp. MEMEA*, Bari, Italy, May 2011, pp. 628–631.

[41] J. M. Kasson and W. Plouffe, "An analysis of selected computer interchange color spaces," *ACM Trans. Graph.*, vol. 11, no. 4, pp. 373–405, Oct. 1992.

[42] M. Sweeney and S. Hochgreb, "Autonomous extraction of optimal flame fronts in OH planar laser-induced fluorescence images," *Appl. Opt.*, vol. 48, no. 19, pp. 3866–3877, Jul. 2009.

[43] A. K. Hamous and M. R. El-Sakka, "SRAD, optical flow, and primitive prior based active contours for echocardiography," in *Proc. Comput. Vis., Imag. Comput. Graph., Theory Appl.*, A. Ranchordas, J. M. Pereira, J. Araujo, and J. M. R. S. Tavares, Eds., 2009, pp. 158–171.

[44] A. R. Smith, "Color gamut transform pairs," *Comput. Graph.*, vol. 12, no. 3, pp. 12–19, Aug. 1978.

[45] R. C. Gonzalez and R. E. Woods, *Digital Image Processing.*, 3rd ed. Upper Saddle, NJ: Pearson Educ. Inc., 2008, pp. 407–414.

[46] K. L. Wuensch, *Skewness, Encyclopedia of Statistics in Behavioral Science 2005*. Hoboken, NJ: Wiley.

[47] H. L. MacGillivray, "Skewness and asymmetry: Measures and orderings," A*nn. Stat.*, vol. 14, no. 3, pp. 994–1011, 1986.

[48] K. Pearson, "Contributions to the mathematical theory of evolution, II: Skew variation in homogeneous material," *Philos. Trans. Roy. Soc. London A, Math. Phys. Sci.*, vol. 186, pp. 343–414, 1895.

[49] [Online]. Available: http://rsbweb.nih.gov/ij/

[50] [Online]. Available: http://www.dentistry.bham.ac.uk/landinig/software/ autothreshold/autothreshold.html

[51] L.-K. Huang and M.-J. J. Wang, "Image thresholding by minimizing the measures of fuzziness," *Pattern Recognit.*, vol. 28, no. 1, pp. 41–51, 1995.

[52] J. M. S. Prewitt and M. L. Mendelsohn, "The analysis of cell images," *Ann. New York Acad. Sci.*, vol. 128, no. 3, pp. 1035–1053, Jan. 1966.

[53] T. W. Ridler and S. Calvard, "Picture thresholding using an iterative selection method," *IEEE Trans. Syst., Man, Cybern.*, vol. SMC-8, no. 8, pp. 630–632, Aug. 1978.

[54] C. H. Li and P. K. S. Tam, "An iterative algorithm for minimum cross entropy thresholding," *Pattern Recognit. Lett.*, vol. 18, no. 8, pp. 771–776, 1998.

[55] J. N. Kapur, P. K. Sahoo, and A. K. C. Wong, "A new method for gray-level picture thresholding using the entropy of the histogram," *Graph. Models Image Process.*, vol. 29, no. 3, pp. 273–285, 1985.

[56] C. A. Glasbey, "An analysis of histogram-based thresholding algorithms," *CVGIP, Graph. Models Image Process.*, vol. 55, no. 6, pp. 532–537, Nov. 1993.

[57] J. Kittler and J. Illingworth, "Minimum error thresholding," *Pattern Recognit.*, vol. 19, no. 1, pp. 41–47, 1986.

[58] W. Tsai, "Moment-preserving thresholding: A new approach," *Comput. Vis., Graph., Image Process.*, vol. 29, no. 3, pp. 377–393, Mar. 1985.

[59] W. Doyle, "Operation useful for similarity-invariant pattern recognition," *J. Assoc. Comput. Mach.*, vol. 9, no. 2, pp. 259–267, Apr. 1962.

[60] A. G. Shanhbag, "Utilization of information measure as a means of image thresholding," *Graph. Models Image Process.*, vol. 56, no. 5, pp. 414–419, 1994.

[61] G. W. Zack, W. E. Rogers, and S. A. Latt, "Automatic measurement of sister chromatid exchange frequency," *J. Histochem. Cytochem.*, vol. 25, no. 7, pp. 741–753, Jul. 1977.

[62] J. C. Yen, F. J. Chang, and S. Chang, "A new criterion for automatic multilevel thresholding," *IEEE Trans. Image Process.*, vol. 4, no. 3, pp. 370–378, Mar. 1995.

Gianluca Sforza received the B.S. degree in computer science and digital communication and the Laurea degree in computer science from the University of Bari "Aldo Moro," Bari, Italy, in 2004 and 2007, respectively, where he is currently working toward the Ph.D. degree in the Computer Science Department, discussing a thesis on techniques for image description.

His research interests include recursion theory, image analysis, and computational intelligence for image retrieval.

Giovanna Castellano received the M.S. and Ph.D. degrees in computer science from the Department of Computer Science, University of Bari "Aldo Moro," Bari, Italy, in 1993 and 2001, respectively.

From 1993 to 1995, she was a Fellow Researcher with the Institute for Signal and Image Processing, consiglio nazionale delle ricerche (CNR), Bari. Since 2002, she has been an Assistant Professor with the Department of Computer Science, University of Bari "Aldo Moro." Her research interests fall in the area of computational intelligence, with special focus on artificial neural networks, fuzzy systems, neuro-fuzzy modeling, granular computing, Web personalization, and fuzzy image processing. Within these research areas, she has been an author of more than 150 papers published on scientific journals and international conference proceedings.

Sai Krishna Arika received the M.S. degree in electrical engineering from Southern Illinois University, Edwardsville, in August 2011.

He is currently with Southern Illinois University. His area of research is related to image processing, robotics, and networks.

Mr. Arika was a recipient of the First Prize Award in national-level robotic competition held at International Institute of Information Technology, Hyderabad, India, in 2007.

Robert W. LeAnder received the M.S. degree in electrical engineering from Southern Illinois University, Edwardsville, and the Ph.D. degree in bioengineering from the University of Illinois, Chicago.

He is an Associate Professor with the Department of Electrical and Computer Engineering, Southern Illinois University. He teaches classes in electrical engineering, including computer vision, image processing, electromagnetics, bioinstrumentation, stochastic processes, and engineering research. His research interests include medical imaging, automatic diagnosis of skin lesions, retinal implant design, bioelectromagnetics, biophotonics, subtle energy phenomena, and clinical nutrition.

R. Joe Stanley (M'99–SM'05) received the B.S.E.E. and M.S.E.E. degrees in electrical engineering and the Ph.D. degree in computer engineering and computer science from the University of Missouri, Columbia.

Upon completing his doctoral study, he served as an Engineering Specialist with Systems & Electronics, Inc., St. Louis, MO, conducting research and development of imaging techniques for medical and postal applications. He is the Associate Chairman for Computer Engineering and an Associate Professor with the Department of Electrical and Computer Engineering, Missouri University of Science and Technology, Rolla. His research interests include signal and image processing, computational intelligence, medical informatics, and automation.

William V. Stoecker received the B.S. degree in mathematics from California Institute of Technology, Pasadena, in 1968, the M.S. degree in systems science from the University of California, Los Angeles, in 1971, and the M.D. degree from the University of Missouri, Columbia, in 1977.

He is an Adjunct Assistant Professor in computer science with the Missouri University of Science and Technology, Rolla, and a Clinical Assistant Professor in dermatology with the Health Sciences Center, University of Missouri. He is CEO of

Stoecker & Associates. His research interests include image analysis techniques for diagnosis of melanoma and skin cancer, medical informatics, and application of engineering methods to diagnostic problems in dermatology.

Jason R. Hagerty received the B.S. degree in computer science and computer engineering from Missouri University of Science and Technology, Rolla, where he is currently working toward the M.S. degree in computer engineering.

He is currently with Stoecker & Associates, Rolla. His area of research is image processing with application in the medical field.

SECTION

2. CONCLUSION

The work presented in this thesis demonstrates that adaptive threshold determination using skewness correction can provide more accurate gray area detection. Based on the metric *INACCURACY,* correction of the estimated histogram asymmetry deviation allows significant improvement of gray area segmentation.

Histograms of gray areas are heterogeneous, with a minority having a blue "tail" skewed primarily to the right. These blue tails likely represent dermatologists' assessment that gray and blue-gray have the same physiology. This assessment includes gray with blue-gray because the gray is at a deeper level in the skin, resulting in appearing bluer in color due to the Tyndall effect. Consequently, a set of images having gray is heterogeneous, with the gray areas in some images having a histogram skewed toward brighter blue. It was concluded that both gray and blue gray are seen in these early melanomas with some images having greater amounts of blue, resulting in a rightward skew.

The presented comparative results show that thresholding without the proposed skew correction can lead to great errors in final segmentation. Correct segmentation of these regions depends entirely upon histogram analysis, and it is therefore quite sensitive to skew distortion of the image histograms. Further research could combine the presented histogram analysis with one or more existing thresholding methods and or machine learning algorithms to provide further improvements in existing segmentation results and possible diagnosing of MIS.

The task of gray area segmentation comprises an incremental step toward the development of an automatic diagnostic system capable of detecting the early stages of melanoma from a set of features extracted from dermoscopic images.

VITA

Jason Richard Hagerty was born in Fort Leonard Wood, Missouri. In May 2000, he received a Bachelor of Science degree in Computer Science with a minor in Mathematics from the University of Missouri-Rolla, Rolla, Missouri. He took a full time position with S&A Technologies of Rolla, Missouri developing techniques and algorithms to diagnose skin lesions given a dermoscopic image. Wanting to further increase his knowledge in the fields of computer vision and machine learning he returned to school and in May of 2011 he received a Bachelor of Science degree in Computer Engineering from Missouri University of Science and Technology, Rolla, Missouri. That same year, he was accepted into the Computer Engineering graduate program at Missouri University of Science and Technology. In May 2016 he received his MS degree in Computer Engineering from Missouri University of Science and Technology. Upon completion of the requirements for a MS degree he will pursue a PhD in Computer Engineering at his alma mater.